CFD Simulation of Airflow and Temperature Field in Room with Convective Heat Source

Weizhen Lu[†‡] Andrew T Howarth[‡] C M Tam[†] A P Jeary[†]

† Department of Building & Construction, City University of Hong Kong, 83 Tat Chee Kowloon Tong, Kowloon, HONG KONG

‡ Department of Building Studies, School of The Built Environment, De Montfort University, Leicester LE1 9BH, UK

Abstract

A CFD simulation of airflow and temperature field in a heated room has been described in the paper. The tracking of pollutant particle movement is also presented here. The comparisons between computation and experiment show good and acceptable agreement. It can be concluded that CFD prediction can capture the main features of convective flow and provide satisfactory results. It can be seen that the thermal wall jet created by radiator greatly influences airflow pattern, temperature and pollutant particle distribution in the heated room. It can also be seen that the area close to the heat source takes high risk of air-born contamination and imposes harmful effect to the occupant.

Nomenclature

A	constant
B	constant
B_i	body force of fluid experienced(N/m^3)
C	constant or turbulent constant
d_p	particle diameter (μm)
E	constant, E≈9.0
f	function
G_k	turbulent generation term
G_B	buoyancy term
g	gravitational acceleration (m/s^2)
H	enthalpy (J/kg); Height (m)
k	turbulent kinetic energy (m^2/s^2)
L	length (m)
P_r	molecular Prandtl number $\left(P_r = \frac{\mu C_p}{\lambda}\right)$
p	pressure (N/m^2)
Q	heat flux (W/m^2)
R_e	Reynolds number $(R_e = \frac{\rho V d}{\mu})$
R_f	Richardson number (R_f=-G_B/G_k)
R_{si}	thermal resistance of inside surface ($W^{-1}\cdot m^2\cdot K$)
$S_{\phi i}$	source term in governing equation
T	temperature (K or °C)
T_w	wall temperature (K or °C)
T^+	scaled wall temperature
U	fluid velocity vector **U**=(u, v, w)
U	velocity component (m/s), thermal transmittance ($W\cdot K^{-1}\cdot m^{-2}$)
u^+	scaled velocity parallel to wall surface
V	velocity component (m/s); volume of space (m^3)
W	velocity component (m/s)
x, y, z	co-ordinates or distance (m)
y^+	scaled distance to the wall surface

Greek symbol

β	compressibility coefficient (K^{-1})
ϕ_i	dependent variable of general equation
Γ_Φ	diffusive coefficient in general equation
ε	turbulent energy dissipation rate (m^2/s^3)
κ	von Kármán constant, κ=0.4~0.44
λ	thermal conductivity of fluid (W/m·K)
μ	dynamic viscosity of fluid (kg/m·s)
μ_t	turbulent dynamic viscosity of fluid (kg/m·s)
ρ	density of surrounding fluid (kg/m^3)
ρ_p	density of particle (kg/m^3)
σ_t	constant, σ_t=0.71
σ_H	Prandtl number of H
σ_k	Prandtl number of k
σ_T	turbulent Prandtl(Schmidt) number
σ_ε	Prandtl number of ε
τ_{wi}	wall shear stress (N/m^2)

I. Introduction

Air movement in a building or a room is normally caused by thermal or momentum differences between the warm and cold zones (natural convection), by mechanical ventilation system (forced convection) or by a combination of both. Natural convection is very common in a room, e.g. winter heating. In practice, a typical winter heating case is when a cold surface (window) is located above a hot surface (radiator). The distributions of air movement, temperature, and turbulence intensity and heat transfer induced by such heat source play a crucial role to the thermal comfort, the indoor air quality and the energy conservation. This type of flow is very unstable and depends on many factors, e.g. the conditions of room surfaces, the strength and the size of heat source, etc. Few experimental data can be found, in the literature, to measure natural convective flow [1-5].

Computational Fluid Dynamics provides a cost effective method to predict the whole flow field in buildings[6-11]. The use of CFD method to simulate air movement in buildings has contributed to the understanding of airflow in buildings. Studies have also shown that CFD application in building engineering is associated with certain shortcomings, e.g., limitation of simulation of full-scale, three-dimensional buoyant flow, prediction of pollutant particle distribution under buoyancy effect, etc. The research reported here includes: a. To use CFD to predict a three-dimensional airflow field and temperature distribution in a full-scale enclosure with a radiator. The predicted airflow pattern and temperature field will be validated by the measured data carried out by Lebrun[4] and Howarth[5]; and, b. To use CFD to predict smoke particle distribution in the room[12].

II. Physical Description

The physical phenomenon studied by Lebrun[4] & Howarth[5] is a full-scale test chamber shown in figure 1. The relevant parameters are: Room L×H×W=4.74×2.7×3.45m³ Window h×w=1.6×2.2m², Radiato h×w=0.6×1.1m² (effective heat flu 440W/m²). The flow domain is divided int 33x20x23 cells and the mesh scheme is show in figure 2. The chamber was lined with sor of insulating materials. The experiment wa carried out by measuring the temperatures a certain sample points within the room[4][5]. Th outside environmental condition is winte season ($t_o = -3°C$). The average ai temperature in room is t_{ai}=22°C. The physica properties of room air are calculated based o the value of t_{ai}.

III. Mathematical Model

The mathematical descriptions of airflow ar based on the fundamental laws of physics, i.e. mass, momentum and energy conservation etc. These equations can be expressed in th following general formation:

$$\frac{\partial}{\partial t}(\rho\phi_i) + \mathrm{div}\left(\rho V\phi_i - \Gamma_{\phi_i}\mathrm{grad}\phi_i\right) = S_{\phi_i} + S_{\text{Buoyancy}} \quad (1)$$

where $S_{\phi i}$ represents all source terms excep the buoyancy term. The attention, in thi study, is turned to the convective heat transfe flow, in which buoyancy force plays a majo role because it is the source of energy for th mean motion itself. Such movement i produced under gravity by a density contras between the source fluid and its surroundin fluid. From the above general equation, it ca be seen that buoyancy effect affects the flo field through the formation of source term i general equation. The standard k-ε turbulenc model is applied to simulate the turbuler characters in this study.

Certain expressions of this phenomenon i needed to describe the buoyancy effect. Th buoyancy term, $-\rho\beta g\theta$, can be expressed:

$$-\rho\beta g\theta = -\rho\beta g(T - T_o) \quad (2)$$

where T_o is the reference temperature which i normally chosen as a ' mean temperature ' i some sense; e.g., the bulk temperature of th room air.

An extra generation term, due to the buoyancy effect, should be included in the source terms of turbulent equations of k and ε which, based on Boussinesq approximation, is defined as:

$$G_B = -\beta g \frac{\mu_t}{\sigma_H} \frac{\partial \theta}{\partial y} \qquad (3)$$

The constants appearing in the k-ε two-equation model are assigned the values recommended by Launder & Spalding[18].

IV. Boundary conditions imposed on flow simulation

1. Boundary conditions for velocity

The general formula for velocity on wall takes the following form:

$$A_i U_i + B_i \tau_{wi} = C_i, \qquad i = 1,2,3 \qquad (4)$$

In this study, the non-slip condition at all solid surfaces, including radiator surfaces, is applied for all velocities, then $A_i = 1$, $B_i = C_i = 0$, i.e., $U_w = V_w = W_w = 0$.

2. Boundary conditions for temperature

The room is not well insulated and heat losses exist due to the temperature differences between inside and outside. The heat transfer boundary condition at the wall surface can be expressed in a general form as below:

$$A_w T_w + B_w Q_w = C_w, \; Q_w = \left(\lambda \frac{\partial T}{\partial n}\right)_w \qquad (5)$$

Here A, B and C are non zero values. According to CIBSE Guide, the heat loss through wall unit relates to the temperature difference on both sides of the wall, the thermal transmittance of wall (U-value) and the thermal resistance of inside wall surface R_{si}. So A, B and C take the following values:

$$A_w = 1, \qquad B_w = \frac{1}{U} - R_{si}, \qquad C_w = T_o \qquad (6)$$

3. Boundary conditions for turbulent flow

A special method, wall function approach for treatment of turbulent characters in near wall region, is necessary for turbulent flow due to the damping effect of wall surfaces. The wall function approach assumes that the flow in near-wall region can be generally divided into a laminar and a turbulent region. Three scalar variables, i.e., scalar velocity u^+, scalar co-ordinate y^+ and scalar temperature T^+, have been defined in wall function approach. Let y_o^+ denotes the joint point of the laminar and turbulent region (for smooth wall surface, $y_o^+ = 11.6$), then the wall function can be expressed as below:

$$u^+ = \begin{cases} y^+ & y^+ < y_o^+ \\ \dfrac{1}{\kappa} \ln(Ey^+) & y^+ > y_o^+ \end{cases} \qquad (7)$$

$$T^+ = \begin{cases} \sigma_l y^+ & y^+ < y_o^+ \\ \sigma_T \left[u^+ + f\left(\dfrac{P_r}{\sigma_T}\right) \right] & y^+ > y_o^+ \end{cases} \qquad (8)$$

$$\varepsilon = \frac{C_\mu^{3/4} k^{3/2}}{\kappa y} \qquad (9)$$

V. Results and Analysis

The results of numerical simulation of airflow and temperature field in the case can be obtained by solving the above equation set. The computations are carried out by using a commercial CFD code, CFDS-FLOW3D. The numerical results are expressed as below:

1. Airflow field

Figure 3a, b and c represent the airflow patterns in different planes along the room width. A thermal rising wall jet is produced along the window surface above the radiator in the centerline plane (figure 3b). The jet develops into a convective thermal boundary layer along the surface and entrains cold air from surroundings. The air in the hot plume flows upwards along the surface and then deflects when it reaches the ceiling. The air movement under the ceiling surface is rather complex. The airflow develops into a ' buffer zone ' under the ceiling. Some of the hot air flow along the ceiling surface and some

disperse downwards due to heat exchange. A large air circulation is formed under the ceiling due to the mixing of hot and cold air. The main flow direction in the occupied zone, i.e., under the ' buffer zone ', is towards the hot surface due to the entrainment of the jet. A downdraught flow is formed at the cold surface opposite to the radiator. The airflow patterns in the planes besides the central plane are shown in figures 3a and 3c. It can be seen that the flow is symmetrical about the centerline plane. The air movement in those planes are separated into two main regions — the upper warm counter clockwise circulation and the lower cool clockwise circulation. The flow between these two regions is mainly towards the hot wall jet. The entrainment of cold air from the surrounding and disperse of hot air to the room space complete the air circulation and the heat exchange.

Figure 4 presents the observed air movement in central plane by Howarth[5] using a flow visualization technique. The rising convective hot plume (A) flows upwards into a ' buffer zone ' (B & C) under the ceiling. The air then disperses downwards into the core (D) of the room to be subsequently entrained into the rising boundary layer, so completing its circulation. Comparing fig. 3b with fig. 4, it can be seen that the airflow patterns between prediction and experiment are very similar. It also shows that the CFD simulation can capture the main flow features and provide acceptable results.

2. Temperature field

The temperature distributions in the room space are presented in figure 5. The figure demonstrates the development of thermal boundary layer along the window surface and its dispersion sketch. The temperature field presents stratified characteristics along the room height. The maximum temperature difference from ankle level (0.1m) to head level (1.8m) is about 2°C and meets the thermal comfort criteria according to CIBSE Guide. A temperature swamp from the radiator to the window surface can be observed from figure 5.

The comparisons of temperature field between simulation and measurement are presented in figure 6 (centerline plane at z=1.725m) and 7 (side plane at z=2.5875m). Generally, the numerical results show good agreement with the relevant measured values. It can be seen that numerical simulation produces satisfactory results. Some discrepancies exist between computation and experiment. The following reasons may cause the errors: a. the mesh used in the simulation is not fine enough and needs to be further refined; b. the turbulence model used may need to be improved, e.g. low-Reynolds number k-ε model, Reynolds-stress model, etc.; c. the measurement may not be accurate enough due to the limitation of accuracy of instrument.

3. Particle movement

Figure 8a, b, c and d present the particle tracking routes in the room. A smoking source is assumed to be located in the middle of the room. The particles are represented by certain sample particles with size ranging from 1μm to 20μm. From these figures, it can be seen that all particles are moving towards to the hot plume first due to the entrainment of the thermal jet. The particles go up with the hot air once they are entrained into the hot jet and then disperse into the room space. It is interesting to notice that small particles (d_p<10μm) mainly suspend or deposit in upper warm zone (see fig. 8a and 8b) due to the buoyancy effect (i.e., the density difference induced by buoyancy effect), while large particles (d_p>10μm) disperse through the whole room space and finally deposit on the floor or vall surfaces. Those particles deposit on the ceiling or wall surfaces impose the possibility of soiling problem, e.g., the wall surface close to the radiator takes the higher chance to be contaminated by smoking particles than other wall surfaces due to the large amount of particles entrained to the hot plume above the radiator. In practice, this phenomenon can be observed that the internal surface close to the radiator becomes yellow gradually. Figure 8 shows that particles are more concentrated in the area close to the heat

source than the others. That means the occupants sitting close to the radiator take higher possibility of passive smoking than those sitting at the other side of the pollutant source. Those particles dispersed in the room space significantly influence the indoor air quality. From figure 8, it can be seen that the thermal wall jet flow produced by the radiator greatly influences the pollutant particle movement and distribution in the room. Figure 8 also implies that the method to improve the indoor environment is to install an extracted fan at the ceiling which may remove the smoking particles from the room effectively and maintain the acceptable indoor air quality.

VI. Conclusions

A CFD modeling of convective airflow and particle movement in a room heated by a radiator has been presented in this paper. The following remarks emerge:

1. The thermal wall jet created by radiator greatly influences the airflow pattern, temperature distribution and pollutant particle movement. The simulated and observed airflow patterns are very similar. The CFD simulation captures the main flow features;
2. The predicted temperature results show good agreement with the measured data;
3. The thermal wall jet also affects the particle movement in room space. Small particles are likely to suspend in the upper warm zone or deposit on the high level of internal surfaces; while large particles travel through the room space and deposit on the floor level;
4. The area close to heat source takes higher risk of air-born contamination and imposes harmful effect to occupants in that area;
5. Further study is required to improve the accuracy of CFD simulation, e.g. turbulence model, accurate description of pollutant source, etc.

VII. References

1. Cheesewright R. (1967) Natural convection from a plane vertical surface in non-isothermal surroundings. Int. J. Heat Mass Transfer, 10, 287-309.
2. Brown, W. G. and Solvason, K. R. (1962) Natural convection through rectangular opening in partitions, part 1: vertical partition, International Journal of Heat & Mass Transfer, 5, 859-868.
3. Shaw, B. H. (1972) Heat and mass transfer by natural convection and combined natural and forced air flow through large rectangular openings in vertical partition, Proc. Int. Mech. Eng. Conf. on Heat & Mass Transfer by combined forced & natural convection, Manchester, 1, 819-831.
4. Lebrun J. & Marret D. (1976) Convection exchanges inside a dwelling room in winter, International Seminar of ICHMT, Dubrovnik, Yugoslavia, September.
5. Howarth, A. T. (1985) The prediction of air temperature variations in naturally ventilated rooms with convective heating, BSER & T, 6(4), 169-175.
6. Nielson, P. V., Restivo, A. and Whitelaw, J. H. (1979) Buoyancy affected flows in ventilated rooms, Num. Heat Transfer, 2, 115-127.
7. Markatos, N. C., Malin, M. R. and Cox, G. (1982) Mathematical modelling of buoyancy-induced smoke flow in enclosure, Int. J. Heat & Mass Transfer, 25, 63-75.
8. Chen, Q., Moser, A. and Huber, A. (1990) Prediction of buoyant, turbulent flow by a low-Reynolds-number k-ε model, ASHRAE, 96, pt 2, 564-573.
9. Moser, A. 1992 Numerical simulation of room thermal convection , - Review of IEA Annex-20 results, Int. Symp. of Room Air Convection and Ventilation Effectiveness, University of Tokyo, July 22-24.
10. Jiang, Z., Haghighat, F. and Wang, J. C. Y. (1992) Thermal comfort and indoor air quality in a partitioned enclosure under

mixed convection, Building and Environment, 27(1), 77-84.
11. Jiang, Z., Haghighat, F. and Chen, Q. (1995) Buoyancy effects on air quality in a partitioned office with displacement ventilation. Proc. 'Indoor Air Quality, Ventilation and Energy Conservation in Buildings', 2nd International Conference, Montreal, 1, 435-447.
12. Rodi, W. (1980) Turbulence models and their applications in Hydraulics — a state of the art review. Int. für Hydromechanik, Univ. of Karlsruhe, Germany.
13. Launder, B. E. and Shima, N. (1989) Second-moment closure for the near-wall sublayer: development and application, AIAA Journal, 27(10), 1319-1325.
14. Lu, W. Z. (1995) Modelling of airflow and aerosol particle movement in buildings, Ph.D. thesis, De Montfort University, UK.
15. Lu, W. Z., Howarth, A. T., Adam, N. and Riffat, S. B. (1996) Modelling and measurement of airflow and aerosol particle distribution in a ventilated two-zone chamber, Int. Journal of Building & Environment, 31(5), 417-423.
16. CIBSE Guide, 1986
17. CFDS-FLOW3D Guide, AEA Harwell Laboratory, Didcot, UK, 1994.
18. Launder, B. E. and Spalding, D. B. (1974) The numerical computation of turbulent flows, Computer Methods in Applied Mechanics & Engineering, 3, 269-289.

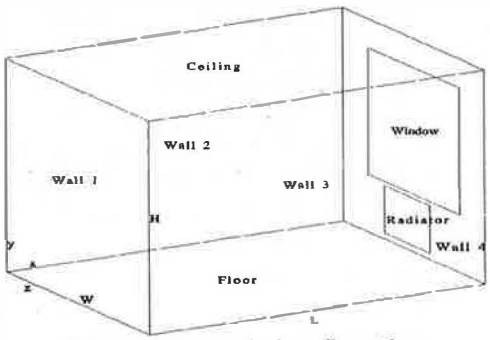

Figure 1 Geometrical configuration

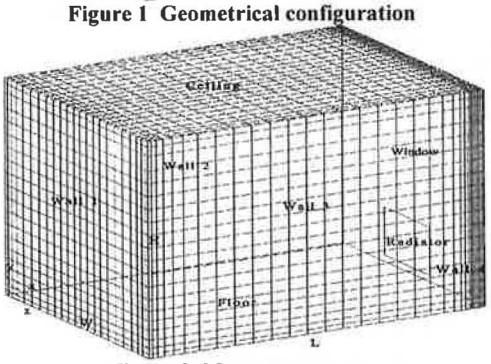

Figure 2 Mesh scheme

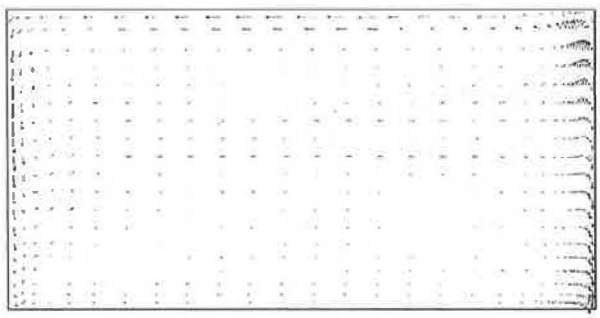

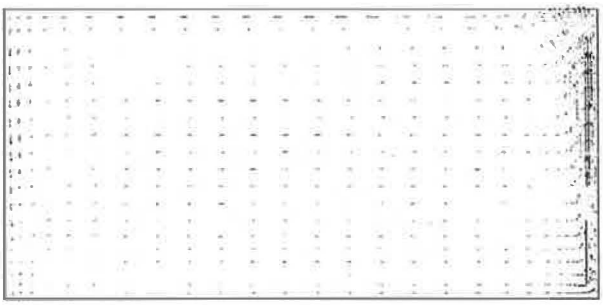

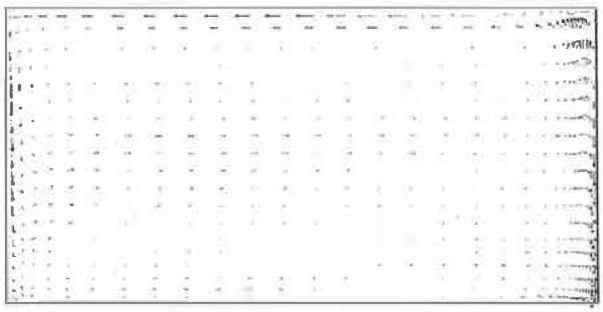

Figure 3a, b & c Airflow patterns in typical planes

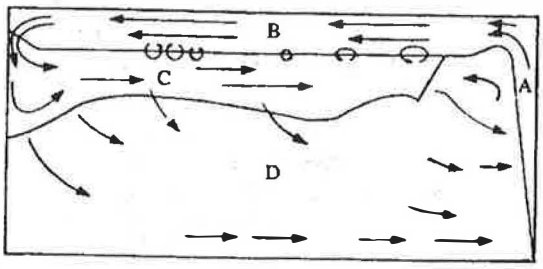

Figure 4 The observed airflow pattern[5]

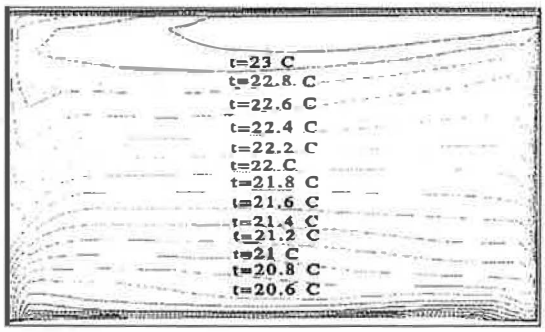

a. Temperature contours in the plane of z=0.8625m

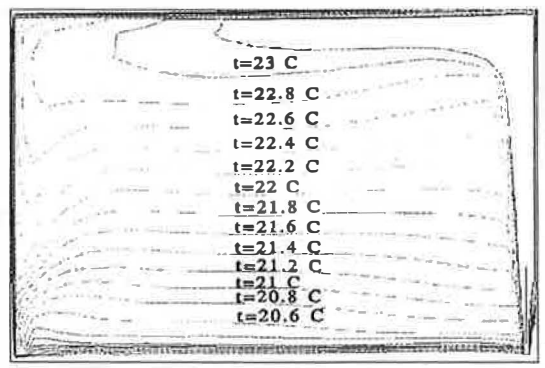

b. Temperature contours in centreline plane (z=1.725m)

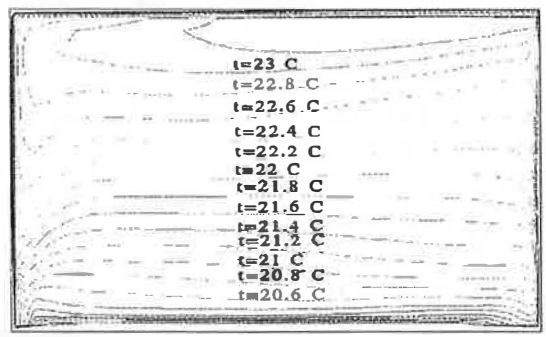

c. Temperature contours in the plane of z=2.5875m

Figure 5 Temperature distributions in typical planes

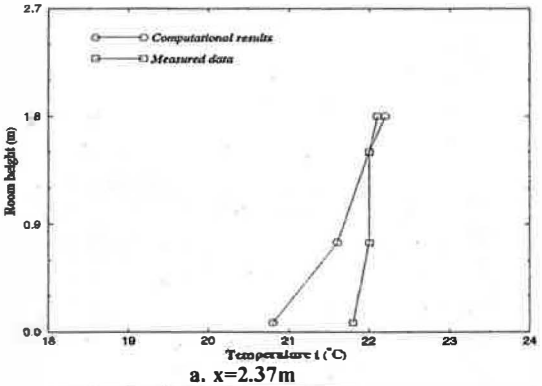

a. x=2.37m

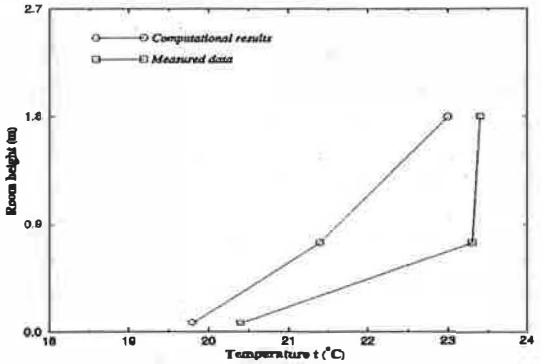

b. x=4.04m

Figure 6 Comparison of temperature in centreline plane

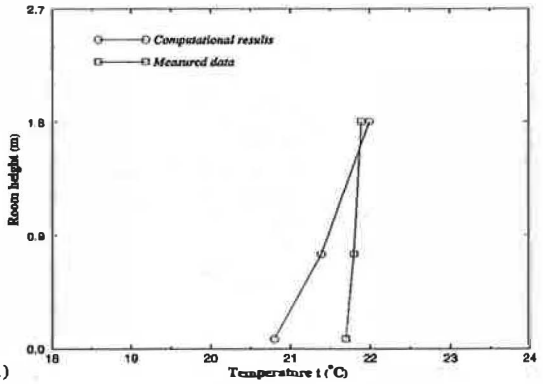

a. x=0.7m

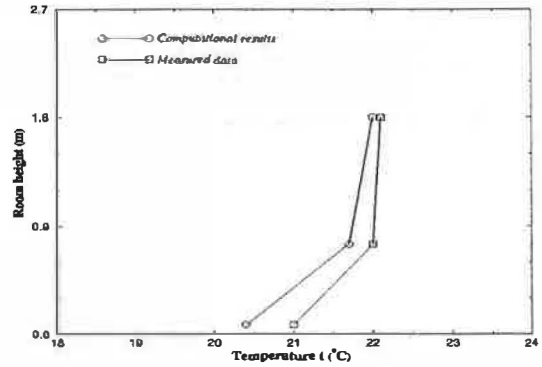

b. x=4.04m

Figure 7 Comparison of temperature in side plane

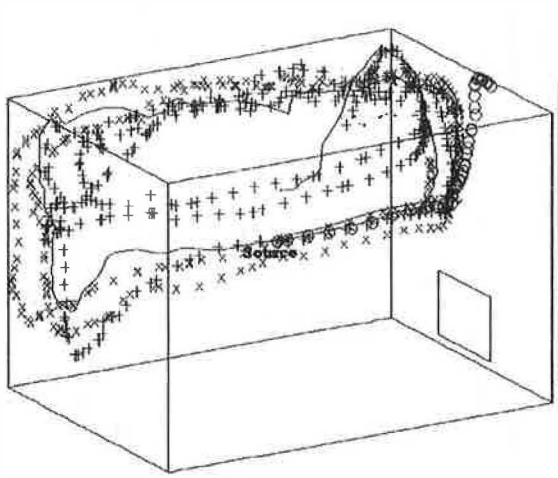

× 1μm + 2μm o 3μm • 4μm – 5μm

Figure 8a Five sample particles tracking in room

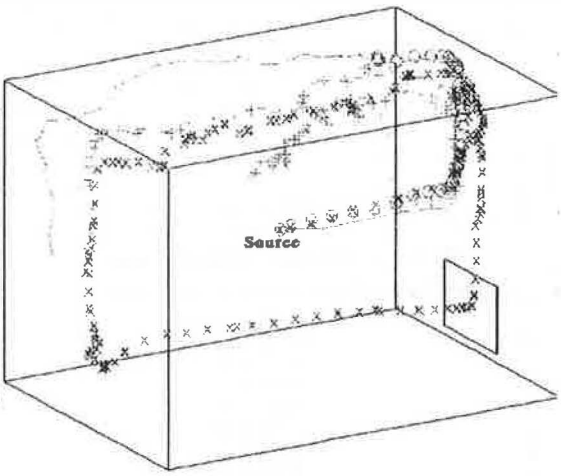

× 6μm + 7μm o 8μm • 9μm – 10μm

Figure 8b Five sample particles tracking in room

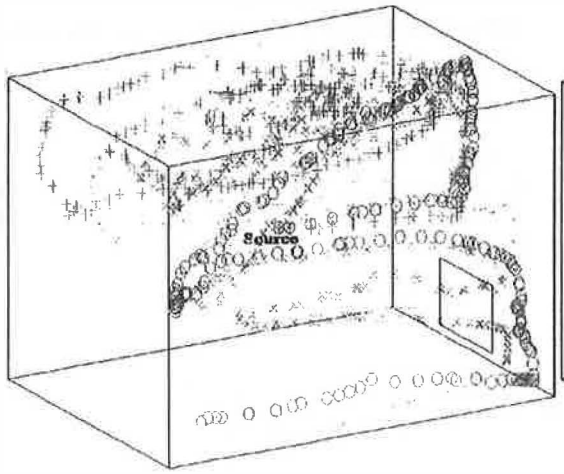

× 11μm + 12μm o 13μm • 14μm – 15μm

Figure 8c Five sample particles tracking in room

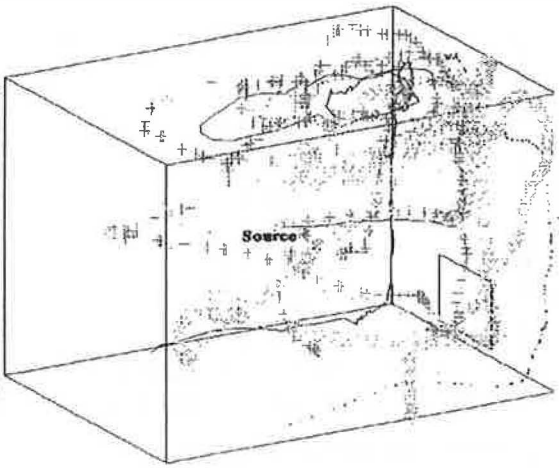

× 16μm + 17μm o 18μm • 19μm – 20μm

Figure 8d Five sample particles tracking in room